

## Self-aligned platinum-silicide nanowires for biomolecule sensing

Fu-Hsiang Ko, Zen-Hou Yeh, Chun-Chi Chen, and Tzeng-Feng Liu

Citation: *Journal of Vacuum Science & Technology B* **23**, 3000 (2005); doi: 10.1116/1.2090967

View online: <http://dx.doi.org/10.1116/1.2090967>

View Table of Contents: <http://scitation.aip.org/content/avs/journal/jvstb/23/6?ver=pdfcov>

Published by the AVS: Science & Technology of Materials, Interfaces, and Processing

---

### Articles you may be interested in

[Detection of electrical characteristics of DNA strands immobilized on self-assembled multilayer gold nanoparticles](#)

*Appl. Phys. Lett.* **89**, 203902 (2006); 10.1063/1.2390653

[Silicon nanowires for high-sensitivity glucose detection](#)

*Appl. Phys. Lett.* **88**, 213104 (2006); 10.1063/1.2206102

[Robust, scalable self-aligned platinum silicide process](#)

*Appl. Phys. Lett.* **88**, 142114 (2006); 10.1063/1.2194313

[Photoelectrochemical deoxyribonucleic acid sensing on a nanostructured TiO<sub>2</sub> electrode](#)

*Appl. Phys. Lett.* **87**, 213901 (2005); 10.1063/1.2135392

[Fabrication and application of long strands of silicon nanowires as sensors for bovine serum albumin detection](#)

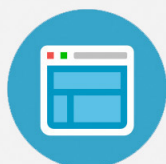
*Appl. Phys. Lett.* **87**, 183106 (2005); 10.1063/1.2123393

---



## Re-register for Table of Content Alerts

Create a profile.



Sign up today!



# Self-aligned platinum-silicide nanowires for biomolecule sensing

Fu-Hsiang Ko,<sup>a)</sup> Zen-Hou Yeh, Chun-Chi Chen, and Tzeng-Feng Liu  
*Institute of Nanotechnology, National Chiao Tung University, Hsinchu 300, Taiwan*

(Received 1 June 2005; accepted 29 August 2005; published 5 December 2005)

A self-aligned platinum-silicide nanowire for biomolecule sensing is developed in this work. The 40 nm nanowire is fabricated through a sequence of electron-beam writing on the polysilicon film, line shrinkage with alkaline solution, platinum film deposition, 550 °C annealing, and aqua regia dissolution. The immobilization of single-stranded capture DNA onto the platinum-silicide nanowire is verified from the fluorescence-labeled technique. The field-effect transistor can distinguish the complementary, mismatched, and denatured DNA via the conductance difference. Although the nanowire sensor has not been integrated into a fluid channel system, we can sense the minimal target DNA concentration down to 100 fM, and the signal is still 1000-fold larger than the noise signal. © 2005 American Vacuum Society. [DOI: 10.1116/1.2090967]

## I. INTRODUCTION

Recently, there has been an increasing demand to find simple and rapid methods for the detection of specific nucleic acids sequences, which can also be used easily in nonspecialized laboratories.<sup>1</sup> The detection of specific DNA sequences is of importance because more than 4000 inherited diseases are known, and much effort is needed to identify the mutations. Most of the traditional techniques in molecular biology are based on hybridization.<sup>2</sup> A single-stranded DNA probe binds to its complementary strand present in a sample, and a double helix structure is built. The degree of hybridization of a complementary probe to the DNA sample is a measure of the amount of that specific sequence in the sample. Typical methods of DNA sensing include optical measurements<sup>3</sup> and electrochemical measurements.<sup>4</sup> Optical measurement is begun by labeling a target DNA with fluorescent material, which reacts to a specific wavelength. By analyzing the manifestation of a fluorescent material with an optical scanner, it is possible to analyze the DNA sequence. Electrochemical measurement is very similar to optical measurement, but the electrochemical signal is extracted from a conventional cell with three electrodes. At present, the use of optical measurements is predominant, but this method requires labeling of fluorescent material and tedious polymerase chain reaction (PCR) to amplify the low-concentration sample.<sup>5</sup> The electrochemical method works well with electric control systems, but it requires an indicator that can bind to a double-stranded DNA selectivity and additional surface preparations.<sup>6</sup>

The concept of using nanowires (NWs) for sensing the molecules has been proposed by Lieber's group since 2001.<sup>7</sup> The nanowire's field-effect nanosensors are very sensitive, label free, and operate in real time for detection of biomolecules. The method flows and aligns the single-crystal boron-doped silicon nanowires, prepared by catalyst-mediated vapor-liquid-solid growth method, onto the source and drain areas. The charge carrier (hole) density in the nanowires can be adjusted by the applied gate voltages and varied with the

molecular attachment. For examples, molecule binding onto the nanowire causes the carrier depletion or accumulation, and can affect the cross-sectional conduction pathway. The use of "state-of-the-art semiconductor technology" guarantees accurate nanowire alignment and the high sensor yield.<sup>8</sup>

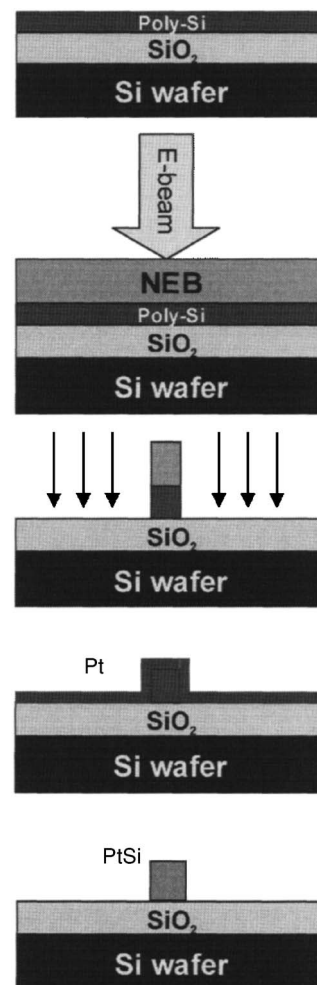
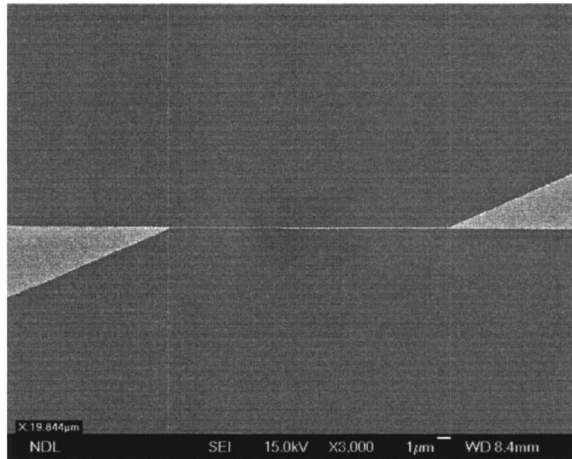
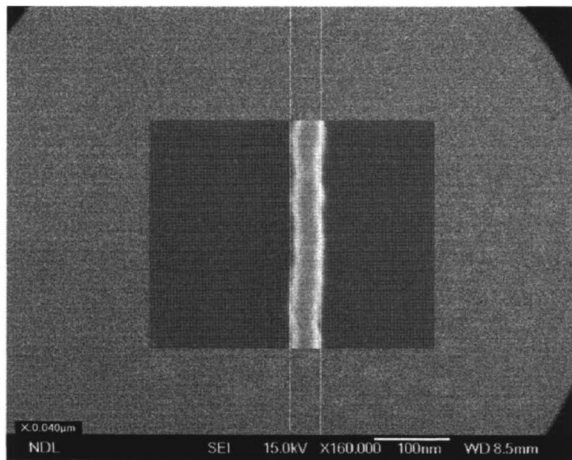


FIG. 1. Fabrication processes for the Pt-silicide nanowire.

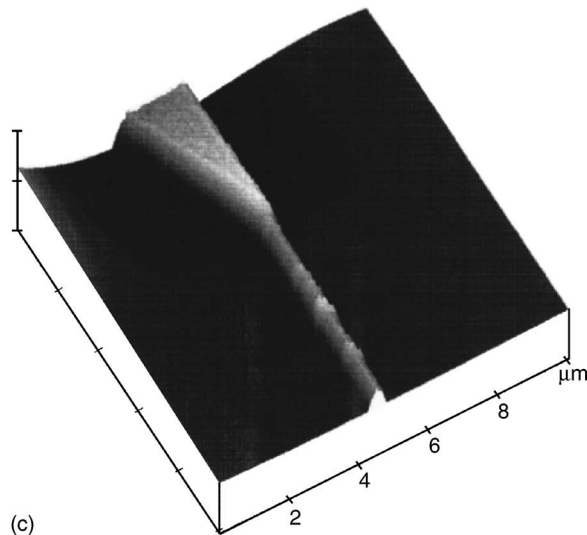
<sup>a)</sup>Electronic mail: fhko@mail.nctu.edu.tw



(a)



(b)



(c)

FIG. 2. (a) 20  $\mu\text{m}$  long Pt-silicide nanowire between source and drain, (b) the 40 nm width of Pt-silicide nanowire, and (c) the three-dimensional AFM image of Pt-silicide nanowire.

The way to overcome the fabricated yield loss and uncontrollable nanowire's assembly site, is to adopt state-of-the-art semiconductor technology. Nanowire fabrication with Pt-silicide film using standard integrated circuit processing has

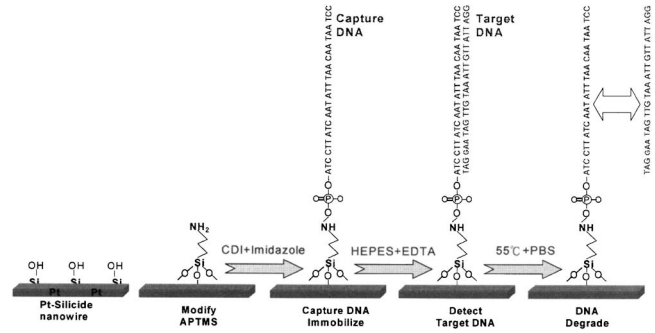


FIG. 3. Various immobilization steps for the DNA molecules on the Pt-silicide nanowires.

not been proposed before to sense biomolecules. Thin films of Pt-silicide exhibit both excellent ohmic as well as Schottky barrier characteristics with *p*- and *n*-type silicon, respectively, and are thus widely used in contact metallization schemes.<sup>9</sup> The typical process for forming Pt-silicide is to deposit Pt thin films on silicon, and then anneal at a suitable temperature to obtain the Pt-silicide phase. The utilization of platinum, which is chemically stable in an oxidizing atmosphere, also possesses the advantage of less toxicity to the attached biomolecules.

In this work, self-aligned Pt-silicide film is formed over the poly-Si nanowire. The conductance under various annealing temperatures, nanowire's lengths and widths are evaluated. Prior to target DNA hybridization, a capture DNA is self-assembled onto the Pt-silicide nanowires. The conductance at the hybridization step, denaturation step, and various target concentrations are also characterized.

## II. EXPERIMENTAL PROCEDURE

There are four steps for the fabrication of DNA sensors; namely, fabrication of poly-silicon nanowire, formation of self-aligned Pt-silicide nanowire, self-assembly of the monolayer of capture DNA onto the Pt-silicide nanowire, and target DNA hybridization and denaturation.

### A. Fabrication of polysilicon nanowire

The basic procedure for the poly-Si gate fabrication is illustrated in Fig. 1. The biosensors were fabricated on 6-in.-diameter,  $\langle 100 \rangle$ -oriented *p*-type Si wafers having a resistivity of 15–25  $\Omega$  cm. All wafers were first cleaned by the standard RCA clean. A 200 nm silicon dioxide layer was thermally grown at 1050  $^{\circ}\text{C}$  for 1 h as the isolation layer. A 100 nm thick poly-Si layer was then deposited at 620  $^{\circ}\text{C}$  in a low-pressure chemical vapor deposition system. The negative electron-beam resist (Sumitomo NEB-22A) was spin-coated on hexamethyldisilazane vapor-primed wafer. The resist was then soft-baked on a hot plate at 110  $^{\circ}\text{C}$  for 120 s. The thickness of the resist film was  $\sim 230$  nm. After exposure on a Leica Wepriint 200 stepper, the wafer was again baked at 105  $^{\circ}\text{C}$  for 120 s. The unexposed resist was developed using the 2.38% tetramethylammonium hydroxide aqueous solution. Again, a hard-bake was applied to the wa-

fer (110 °C for 120 s). The poly-Si pattern was defined using transformer-coupled plasma (TCP) etcher (LAM TCP 9400SE). After defining the 80 nm poly-Si line, the residual resist was removed using ozone and 30 min in SPM solution ( $\text{H}_2\text{O}_2:\text{H}_2\text{SO}_4=3:1$ ). Finally, the standard SC1 process ( $\text{NH}_4\text{OH}:\text{H}_2\text{O}_2:\text{H}_2\text{O}=0.25:1:5$ ) was used to shrink the 80 nm line to 60 nm.

### B. Formation of self-aligned Pt-silicide nanowire

A platinum film of  $\sim 60$  nm was deposited on the 60-nm polysilicon nanowires using ULVAC SBH-3308 RDE sputter system. The Pt film thickness was 59.4 nm. These wafers were then annealed at various temperatures using the Heat-Pulse 610 rapid thermal annealing (RTA) system under 1 atm  $\text{O}_2$  ambient to form the Pt-silicide film across the poly-Si nanowire. The resulting wafers were immersed in aqua regia ( $\text{HNO}_3:\text{HCl}:\text{H}_2\text{O}=1:3:4$ ) at 75 °C to selectively remove the unreacted Pt film without etching oxide, or the underlying metal silicide. Figure 2(a) shows the 20  $\mu\text{m}$  long Pt-silicide nanowire defined between source and drain, and Fig. 2(b) shows a minimal width of 40 nm. This observation suggested that the silicide process could further shrink the nanowire width up to  $\sim 30\%$ . The atomic force microscope (AFM) morphology in Fig. 2(c) also illustrates the fabrication of Pt-silicide nanowire using the standard semiconductor process.

### C. Self-assembly of the monolayer of capture DNA onto the Pt-silicide nanowire

The silanol group ( $\text{Si}-\text{OH}$ ) was formed onto the Pt-silicide due to high oxidant aqua regia to remove the unreacted Pt film mentioned above. Since the silanol group was a good proton donor ( $\text{H}^+$ ) and acceptor ( $\text{Si}-\text{O}^-$ ), the 3-aminopropyl-trimethoxysilane (APTMS) molecule was designed to self-assemble a monolayer onto the Pt-silicide surface. The nanowire sample was immersed into 10% APTMS aqueous solution for 30 min at 37 °C which was adjusted to pH 3.5 with hydrochloric acid. The sample was then rinsed with de-ionized (DI) water and dried on a hot plate. Figure 3 illustrated the terminal amino group was observed from the surface. A selective immobilization technique proposed by Ghosh *et al.*<sup>10</sup> was used to bind the terminal 5' phosphate group of the oligonucleotide to the amino group on the nanowire surface. The procedure was preparing a solution of water-soluble 0.1 M N-cyclohexyl-N'-[2-(N-(methylmorpholino)-ethyl)-carbodiimide-4-toluene sulfonate (CDI) and 0.1 M imidazole. The 1  $\mu\text{M}$  capture DNA was prepared, and then diluted with 0.1 M CDI and imidazole solution to 1 nM capture DNA. The above 100  $\mu\text{L}$  capture DNA solution was dropped onto the Pt-silicide nanowire and reacted for 1 day to ensure the effective immobilization. Then, DI water and PBS solution (i.e., 0.3 M NaCl and 10 mM  $\text{NaH}_2\text{PO}_4/\text{Na}_2\text{HPO}_4$ , pH 7) was used to wash the wafer followed by drying with a hot plate. In order to ensure the effectiveness of capture DNA binding, a fluorescence-labeled single-stranded DNA was also prepared, and followed with the above immobilization process.

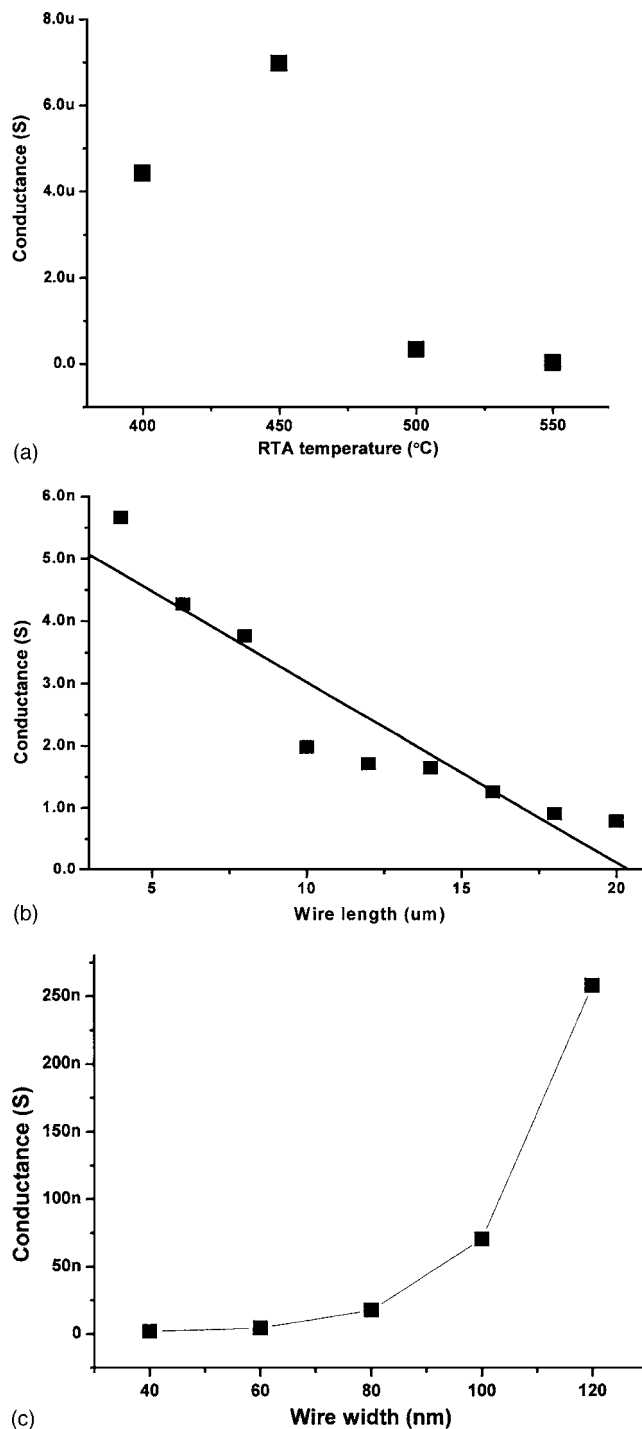


Fig. 4. Effect of (a) annealing temperature, (b) nanowire length, and (c) nanowire width on the conductance.

### D. Target DNA hybridization and denaturation

After surface modification and capture DNA binding, another strand of DNA, namely the target DNA, was applied to hybridize with the capture DNA. The sequence of target DNA in Fig. 3 was complementary to capture DNA. The 10 mM 4-(2-hydroxyethyl)-1-piperazineethanesulfonic acid (HEPES, J.T. Baker Chem. Co.) solution was prepared. A 5 mM ethylenediaminetetraacetic acid buffer was used to ad-

just the HEPES solution to pH 6.6. The 27-mer target DNA was deacrated in the prepared HEPES buffer. Next, the wafers were immersed in the above target DNA solution for 4 h at room temperature, followed by washing with the 0.3 M PBS buffer to remove excess target DNA and dried under N<sub>2</sub>. The resulting chip was washed with 0.3 M PBS buffer to ensure the target DNA and capture DNA hybridization. The chips were then immersed in de-ionized water for 2–3 s, dried with N<sub>2</sub> purge, and put into a low vacuum chamber for preservation. The electrical behaviors of the DNA sensors were characterized using the HP 4156A semiconductor parameter analyzer. After electrical measurement was done, the chips were again washed by 55 °C PBS buffer solution to denature the double stranded DNA previously hybridized. Prior to the electrical measurement, the sample was dried with N<sub>2</sub> purge.

### III. RESULTS AND DISCUSSION

#### A. Optimization for the nanowires

Prior to sample measurement, the noise level of the electrical analyzer is estimated to be 50 fA at 1 V applied, and the noise level for the conductance measurement is about 0.05 pS. The RTA temperature is a crucial parameter to affect the conductance of the Pt-silicide nanowires. Figure 4(a) depicts the effect of annealing temperature on the nanowire's conductance. It was found that the 450 °C annealing exhibited the highest conductance, the smallest contact resistance, and the lowest sheet resistance. The conductance following annealing at 500 °C and 550 °C abruptly decreased to less than 0.05 μS. Naem<sup>11</sup> has proposed that the grain size of Pt-silicide increases with the annealing temperature and time. The high-temperature anneals not only activate the silicide grain growth, but also deteriorate the interface. The formation of grain boundary for the Pt-silicide nanowire can produce high-energy barriers, lowering the conductance.

The length and width of the silicide nanowires are also important factors affecting the conductance. Figure 4(b) shows that the conductance of the fabricated Pt-silicide

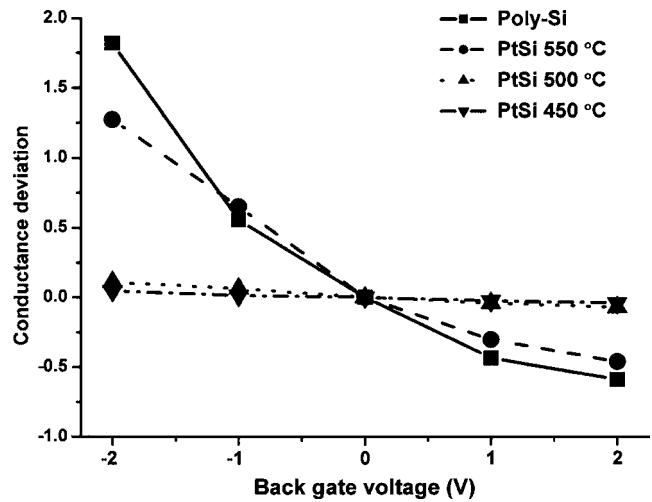


FIG. 5. Conductance deviations for poly-Si nanowire and Pt-silicide nanowires under three annealing temperatures with various stressing voltages.

nanowires linearly decreases with wire length. This result suggests that the Pt-silicide nanowires exhibit the ohmic and conductive characteristics, and can be further used to probe the biomolecules. It is noted from Fig. 4(c) that the conductance abruptly decreases with shrinking of the wire width to the nanoscale. This phenomenon may be attributed to the formation of Pt-silicide grain on the nanowire mentioned above. The lowest conductance signal in Fig. 4(c) is about 0.8 nS for a 40 nm nanowire, and is estimated to be 16 000-fold higher than the noise conductance. Basically, the smaller wire width is more sensitive to the binding molecule.

As we know, the phosphate moiety of the DNA possesses a negative charge, and the binding of DNA molecule onto the Pt-silicide nanowire can influence the charge distribution and change the nanowire's conductance. How does the Pt-silicide nanowire behave compared to the poly-Si nanowire? We deposit the Al back gate to form a field-effect transistor and measure the *I-V* curve for poly-Si nanowire and Pt-silicide nanowire devices. The conduction deviation is defined as follows:

$$\text{Conductance deviation} = \frac{(\text{conductance at nonzero voltage} - \text{conductance at zero voltage})}{\text{conductance at zero voltage}}$$

Figure 5 depicts the conductance deviation for various nanowires. The poly-Si nanowire has higher conductance deviation than Pt-silicide nanowires under -2 V stressing. This observation means the poly-Si nanowire is more sensitive to negative bias. However, the signal intensity from the *I-V* curve of the poly-Si nanowire is very weak. The signal-to-noise ratio of the *I-V* curve of Pt-silicide nanowire is about three orders of magnitude higher than that of the poly-Si nanowire. Hence, the Pt-silicide nanowire with 550 °C an-

nealing is chosen as the candidate nanowire for sensing the charged molecules.

#### B. Sensing of DNA molecule using the Pt-silicide nanowires

A fluorescence-labeled single-stranded DNA is used to ensure the effectiveness of capture DNA binding. As we known if the fluorescence-labeled DNA is not immobilized

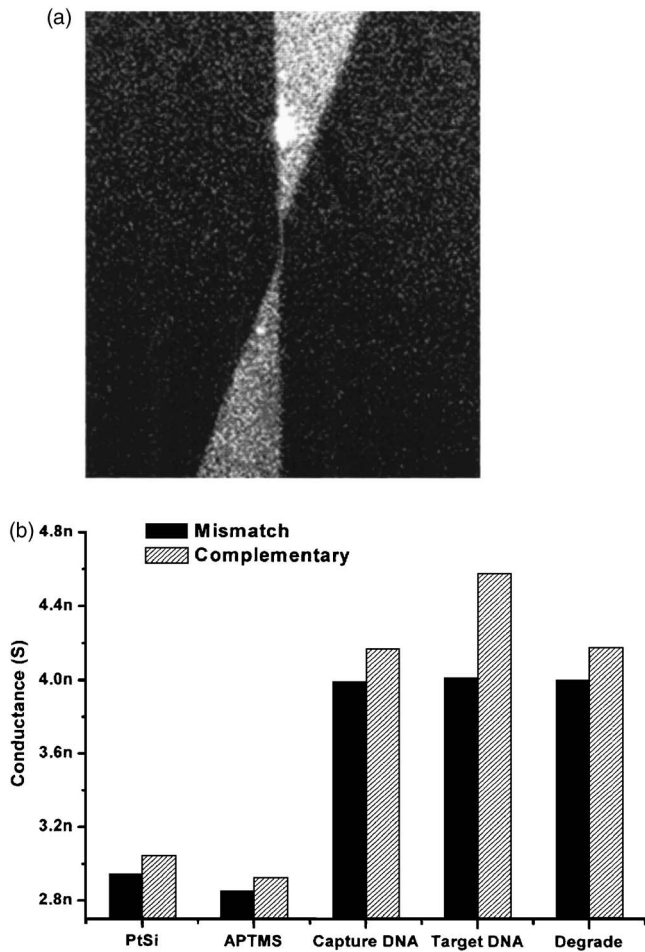


Fig. 6. (a) Fluorescence image of capture DNA, and (b) the conductance of 10 pM complementary and mismatched target DNA on the 6  $\mu\text{m}$  length and 40 nm width Pt-silicide nanowire.

onto the Pt-silicide nanowire, the image cannot be seen in a fluorescence microscope. Figure 6(a) shows the clear image in the fluorescence microscope. The fluorescence-labeled DNA molecule is immobilized onto the source, drain, and the tethering nanowire.

The fabricated 40 nm Pt-silicide nanowire is used to sense the complementary and mismatched DNA molecules. Figure 6(b) illustrates the detection capability of the Pt-silicide nanowires. The immobilization of APTMS molecule onto the Pt-silicide nanowire does not affect the conductance. However, the binding of capture DNA to the terminal amino group can induce the additional hole carriers in the nanowire. The conductance of nanowire is abruptly increased due to the negative charge of DNA molecule. The succeeding hybridization of 10 pM target DNA demonstrates a different conductance for complementary and mismatched DNA. The complementary DNA hybridization can further increase the conductance due to the negative charge character of DNA. On the contrary, the signal of conductance for mismatched DNA is not varied. This observation suggests the Pt-silicide nanowire is a very effective way to distinguish the DNA sequence on the basis of capture DNA design. The Pt-silicide nanowire sensor can be restored in its conductance after

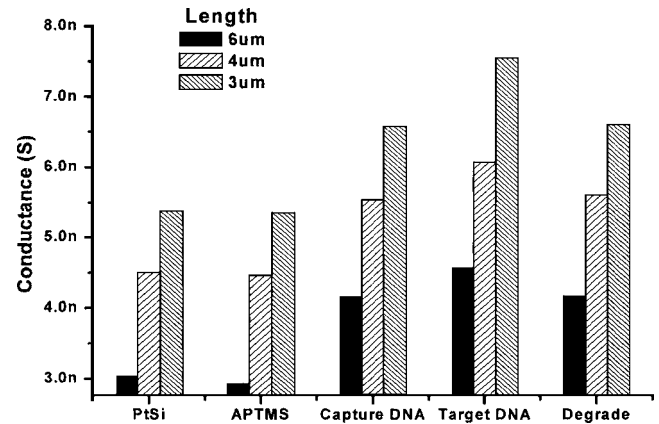


Fig. 7. Conductance for various lengths of Pt-silicide nanowires at width of 40 nm.

washing with 55  $^{\circ}\text{C}$  PBS buffer solution to denature the double stranded DNA previously hybridized. This finding also suggests the detachment of target DNA from the nanowire surface.

Figure 7 illustrates the conductance for various nanowires at lengths of 3, 4, and 6  $\mu\text{m}$ . These three lengths of nanowire can sense the DNA molecule. Comparing the conductance of capture DNA and target DNA, the nanowire with 3  $\mu\text{m}$  length has a larger net conductance difference ( $\Delta S$ ) than the 4 and 6  $\mu\text{m}$  lengths. Hence, we use the nanowire dimension of 40 nm width and 3  $\mu\text{m}$  length to determine the sensing limit of DNA molecule. The  $\Delta S$  represents the conductance difference of target DNA and capture DNA. Figure 8 shows the relationship of conductance difference with respect to various target DNA concentrations. The minimal target DNA concentration that can be detected is about 100 fM. The conductance difference between target DNA and capture DNA at 100 fM is still up to 50 pS, and is still 1000-fold larger than the noise signal. This better detection capability can be used to detect the ultratrace DNA without further PCR amplification. In addition, the detection limit is also better than the

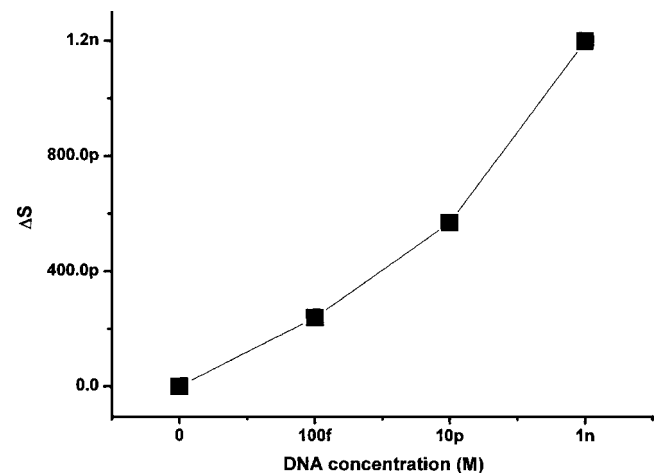


Fig. 8. Relationship of conductance difference with respect to various target DNA concentrations for nanowire of 40 nm width and 3  $\mu\text{m}$  length.

TABLE I. Comparison of various DNA sensing techniques.

|             | Si process Pt-silicide NWs  | SOI process Si NWs   | Microgap Au NPs   | Si process metal oxide-semiconductor field-effect transistor                        |
|-------------|---|--|---|---|
| Reference   | This work   | 8  | 12  | 13  |
| Sensitivity | 100 fM  | 25 pM  | 500 fM  | 1 nM  |
| Advantage   | 1. Standard semiconductor process<br>2. Very high sensitivity<br>3. Low cost per chip<br>4. Simple readout signal<br>5. Label-free chip | 1. Standard semiconductor process<br>2. High sensitivity<br>3. Simple readout signal<br>4. Label-free chip | 1. High sensitivity<br>2. Simple readout signal<br>3. Low cost per chip<br>4. Label-free chip | 1. Standard semiconductor process<br>2. Simple readout signal<br>3. Label-free chip |
| Drawback    | No  | Too expensive SOI wafer  | Long time on Ag reduction and not real-time sensing   | Poor sensitivity and high cost  |

chip designed with silicon-on-insulator (SOI) nanowire,<sup>8</sup> microgap,<sup>12</sup> and complementary metal oxide semiconductor (CMOS) methods.<sup>13</sup> Table I compares our sensor with the literatures.<sup>8,12,13</sup> The Pt-silicide nanowire offers the advantages of eliminating expensive labeling steps, simplifying the signal readout, using standard semiconductor processes and very high sensitivity.

#### IV. CONCLUSIONS

Pt-silicide nanowire DNA sensors have been fabricated using electron-beam direct writing, line shrinkage, self-alignment of platinum film, and rapid thermal annealing. The advantages of the developed methods include the use of a standard silicon semiconductor process, low cost, simple signal readout, and label-free detection. The conductance of the Pt-silicide nanowire is affected by the length and width of the nanowires. The signal linearly decreases with the wire length, and abruptly increases with the wire width. The behavior of wire width at the nanoscale is attributed to the formation of Pt-silicide grains after annealing. The very sensitive nanowire on target DNA sensing is estimated to be 100 fM, which is better than the literature's SOI nanowire, microgap, and CMOS methods.

#### ACKNOWLEDGMENT

This work was supported by the NSC-funded project (NSC94-2113-M-009-020). The electron-beam exposure and measurements were carried out using the facilities located in the National Nano Device Laboratories and National Chiao Tung University.

<sup>1</sup>M. Skena, *Microarray Analysis* (Wiley, New York, 2003).

<sup>2</sup>K. R. Khrapto, Y. P. Lysov, A. A. Khorlyn, V. V. Shick, V. L. Florentiev, and A. D. Mirzabekov, *FEBS Lett.* **256**, 118 (1989).

<sup>3</sup>U. B. Obaid and G. H. Robert, *Biotechnol. Appl. Biochem.* **26**, 27 (1997).

<sup>4</sup>K. Hashimoto, K. Ito, and Y. Ishimori, *Sens. Actuators B* **46**, 220 (1998).

<sup>5</sup>J. M. Claverie, J. P. Hardelin, R. Legouis, J. Levilliers, L. Bougueleret, M. G. Mattei, and C. Petit, *Genomics* **15**, 13 (1993).

<sup>6</sup>H. Korri-Youssoufi and A. Yassar, *Biomacromolecules* **2**, 58 (2001).

<sup>7</sup>Y. Cui, Q. Wei, H. Park, and C. M. Lieber, *Science* **293**, 1289 (2001).

<sup>8</sup>Z. Li, Y. Chen, X. Li, T. I. Kamins, K. Nauka, and R. S. Williams, *Nano Lett.* **4**, 245 (2004).

<sup>9</sup>A. K. Pant, S. P. Murarka, C. Shepard, and W. Lanford, *J. Appl. Phys.* **72**, 1833 (1992).

<sup>10</sup>S. S. Ghosh and G. F. Musso, *Nucleic Acids Res.* **15**, 5353 (1987).

<sup>11</sup>A. A. Naem, *J. Appl. Phys.* **64**, 4161 (1988).

<sup>12</sup>S. J. Park, T. A. Taton, and C. A. Mirkin, *Science* **295**, 1503 (2002).

<sup>13</sup>D.-S. Kim, Y.-T. Jeong, H.-J. Park, J.-K. Shin, P. Choi, J.-H. Lee, and G. Lim, *Biosens. Bioelectron.* **20**, 69 (2004).